

## Reaction of Li with Alloy Thin Films Studied by *In Situ* AFM

To cite this article: L. Y. Beaulieu *et al* 2003 *J. Electrochem. Soc.* **150** A1457

View the [article online](#) for updates and enhancements.

### You may also like

- [Electrochemical Performance of SiAlSn Films Prepared by Combinatorial Sputtering](#)  
T. D. Hatchard, J. M. Topple, M. D. Fleischauer et al.
- [Tungsten Infused Grain Boundaries Enabling Universal Performance Enhancement of Co-Free Ni-Rich Cathode Materials](#)  
Divya Rathore, Chenxi Geng, Nafiseh Zaker et al.
- [Improving the Capacity Retention of LiCoO<sub>2</sub> Cycled to 4.5 V by Heat-Treatment](#)  
Zhaohui Chen and J. R. Dahn



### Your Lab in a Box!

The PAT-Tester-i-16: All you need for Battery Material Testing.

- ✓ All-in-One Solution with integrated Temperature Chamber!
- ✓ Cableless Connection for Battery Test Cells!
- ✓ Fully featured Multichannel Potentiostat / Galvanostat / EIS!

[www.el-cell.com](http://www.el-cell.com) +49 40 79012-734 [sales@el-cell.com](mailto:sales@el-cell.com)

  
electrochemical test equipment





## Reaction of Li with Alloy Thin Films Studied by *In Situ* AFM

L. Y. Beaulieu,<sup>a,b</sup> T. D. Hatchard,<sup>a,\*</sup> A. Bonakdarpour,<sup>a,\*</sup> M. D. Fleischauer,<sup>a,\*</sup>  
and J. R. Dahn<sup>a,\*,\*,z</sup>

<sup>a</sup>Department of Physics, Dalhousie University, Halifax, Nova Scotia B3H 3J5, Canada

Many intermetallic materials deliver poor capacity retention when cycled vs. Li. Many authors have attributed this poor capacity retention to large volume expansions of the active material. Here we report the volume changes of continuous and patterned films of crystalline Al, crystalline Sn, amorphous Si (a-Si), and a-Si<sub>0.64</sub>Sn<sub>0.36</sub> as they reversibly react with Li measured by *in situ* atomic force microscopy (AFM). Although these materials all undergo large volume expansions, the amorphous phases undergo reversible shape and volume changes. The crystalline materials do not. We attribute this difference to the homogeneous expansion and contraction that occurs in the amorphous materials. Inhomogeneous expansion occurs in the crystalline materials due to the presence of coexisting phases with different Li concentrations. Thin films of a-Si and a-Si<sub>0.64</sub>Sn<sub>0.36</sub> show good capacity retention with cycle number.

© 2003 The Electrochemical Society. [DOI: 10.1149/1.1613668] All rights reserved.

Manuscript submitted November 18, 2002; revised manuscript received April 10, 2003. Available electronically September 19, 2003.

Lithium alloys hold great promise as negative electrode materials for lithium-ion batteries.<sup>1-5</sup> They can have much larger specific and volumetric capacities than the graphite electrodes now used in lithium-ion cells. However, the capacity retention of lithium alloys is not yet sufficient for commercial applications.<sup>5</sup>

There can be several reasons for poor capacity retention. First, crystalline materials, like aluminum and tin, form new intermetallic phases when they are reacted with lithium.<sup>5</sup> The large inhomogeneous volume expansion that occurs in coexisting phase regions is thought to cause particle fracture and electrochemical pulverization. This leads to an inability to maintain electrical contact to the fractured portions of particles and to capacity loss.

Amorphous materials, like a-Si<sub>0.64</sub>Sn<sub>0.36</sub><sup>6-8</sup> and a-Si,<sup>9</sup> appear to show capacity loss for a different reason. Beaulieu *et al.*<sup>6-8</sup> have shown that the volume changes of a-Si<sub>0.64</sub>Sn<sub>0.36</sub> as it reacts with lithium is homogeneous and that 10-30 μm pieces of thin films expand and contract reversibly, without further fragmentation. Thin films of a-Si have also shown reversible morphology changes during cycling.<sup>9</sup> It is our opinion that capacity loss in the amorphous alloys occurs because contact is lost to expanding and contracting particles undergoing large volume changes, not because of the particle fracture that occurs for crystalline materials that form intermetallic phases.

In this paper, we use *in situ* atomic force microscopy (AFM) to examine the morphology changes that occur in crystalline and amorphous materials as they react with lithium. Crystalline samples of Sn and Al and amorphous samples of a-Si and a-Si<sub>0.64</sub>Sn<sub>0.36</sub> are the focus. Electrodes made from patterned thin films are used so that the length, width, height, and volume as well as the surface morphology of electrode material particles can be monitored during repeated charge-discharge cycling. We observe a profound difference between the behavior of crystalline and amorphous samples.

Recently, the reaction of Li with Sn has been revisited and found to be more complicated than originally believed.<sup>10-13</sup> It has been shown that during the early stages of cycling, the reaction of Li with Sn can be accompanied by an anomalous irreversible capacity. This irreversible capacity has been attributed to the formation of a foreign film via an electrolyte decomposition process on the surface of the Sn electrode. Using a method suggested by Beattie *et al.*, this irreversible capacity has been eliminated and the changes in morphology of Sn electrodes can be monitored.<sup>13</sup>

Unlike Sn, the reaction of Li with a-Si has not been studied in depth. Due to its low conductivity, a-Si may not be a good candidate

as an anode material for lithium-ion batteries. However, the combination of Si and Sn to form a-Si<sub>0.64</sub>Sn<sub>0.36</sub> creates an anode material capable of delivering large capacities over many discharge/charge cycles.<sup>7</sup> In recent work<sup>6</sup> it has been shown that a-Si<sub>0.64</sub>Sn<sub>0.36</sub> films can reversibly react with lithium to undergo large volume changes over many discharge/charge cycles. Although the film cracks during the first discharge to form well-separated particles, each particle does not experience any further cracking. This means that each particle remaining well adhered to the substrate can expand and contract freely as lithium is inserted and extracted. As shown in Ref. 6, this process can happen for many cycles.

The reason for the good cycling capability of this material is thought, in part, to be attributed to the absence of phase transformations undergone by most tin-containing materials.<sup>7</sup> From the electrochemical data, the reaction of Li with a-Si<sub>0.64</sub>Sn<sub>0.36</sub> is believed to be



Based on the crystallographic phases, this reaction is estimated to give volume expansion on the order of 280% (calculated by  $(V_f - V_i)/V_i$ ). However, to our knowledge this volume expansion has not been measured. By monitoring the size and shape of individual particles of patterned electrodes by *in situ* AFM, we are able to measure the volume changes in both a-Si and of a-Si<sub>0.64</sub>Sn<sub>0.36</sub> as they react with Li for the first time.

### Experimental

Samples were made by magnetron sputtering using a Corona Vacuum Coater's (Vancouver, BC, Canada) V3T system. The system holds up to five targets, is turbopumped, and reaches a base pressure of  $5 \times 10^{-8}$  Torr. 2 in. diam targets of Al, Sn, and Si (Pure Tech 99.9%) were used. The sputtering chamber is equipped with a 40 cm diam water-cooled rotating substrate table and a stationary mask platform. Chamber pressure was maintained at 3 mTorr of argon during deposition. The substrate table angular speed was 20 rpm.

Pure Sn was sputter deposited using a dc power supply, operating at 50 W. Pure Al and pure a-Si were deposited using a radio frequency (rf) power supply operating at 200 W. a-Si<sub>0.64</sub>Sn<sub>0.36</sub> was deposited by cosputtering Si (rf at 200 W) and Sn (dc at 25 W).

Continuous films were deposited on highly polished stainless steel disks (10 mm diam, 1.2 mm thick) and Cu foil. The stainless steel disks and Cu foil were bonded to the water-cooled substrate table using 3M brand Y9415 double-sided adhesive tape. In the same sputtering run, patterned electrodes on identical stainless steel disks were made by sputtering through a fine mesh ( $7.6 \times 7.6$  μm openings) with a periodicity of 12.6 μm (SPI supplies, West Chester, PA). The mesh was held in intimate contact with the surface of the substrate using a shop-made assembly. Typically the films were between 0.3 and 0.5 μm thick.

\* Electrochemical Society Student Member.

\*\* Electrochemical Society Active Member.

<sup>b</sup> Present address: Department of Physics, McGill University, Montréal, Quebec H3A 2T8, Canada.

<sup>z</sup> E-mail: jeff.dahn@dal.ca

*In situ* AFM experiments were conducted using a specially built workstation as reported elsewhere.<sup>14</sup> This workstation is composed of an AFM (Molecular Imaging, Phoenix, AZ) housed inside an Ar-filled glove box (Vacuum Atmospheres Corp., Hawthorne, CA). The AFM and sample were maintained at constant temperature using a silicone heater (Watlow, St. Louis, MO). The reactions of Li with Sn, Al, a-Si, and a-Si<sub>0.64</sub>Sn<sub>0.36</sub> were performed in a shop-made wet-cell also reported in Ref. 14. In all electrochemical experiments, Li metal (FMC, North Carolina) was used as both the counter and reference electrode. 1 M LiPF<sub>6</sub> dissolved in equal parts of ethylene carbonate (EC) and propylene carbonate (PC) was used as the electrolyte. A computer-controlled Keithley 236 source-measure unit was used to control the current to the cell and record its potential as a function of time. Composition analysis and scanning electron microscopy (SEM) imaging was performed using a fully automated JEOL JXA-8200 electron microprobe X-ray microanalyzer equipped with an Oxford Link eXL 131 eV energy-dispersive detector. The 1 μm electron-beam was operated at 15 kV and 15 nA. Oxygen analysis was made by wavelength-dispersive spectroscopy (WDS) using the same instrument. The crystalline and amorphous structures of the various samples were confirmed using a Siemens D5000 diffractometer.

### Results and Discussion

*The reaction of Li with Sn.*—Patterned Sn samples were prepared using the method described previously. The deposited films were on average about 300 nm in height and were made up of numerous islands of tin. The tin samples were found to be crystalline by X-ray diffraction. In order to detect the presence of oxygen in the sputtered samples, electron microprobe analysis was performed. Figure 1 shows a compositional analysis of a single patterned tin spot that we call a tin “tower”. Energy-dispersive spectroscopy was used to detect Sn (from the sample), Fe, Ni, and Cr (from the substrate), while WDS was used to detect oxygen. Figure 1a shows an SEM micrograph of a Sn tower as well as the position and approximate size of the electron-beam. Figure 1b shows the atomic percentage of Sn and oxygen in the Sn tower. In this graph the atomic percentages of Ni, Cr, and Fe are not shown. Figure 1b shows there is no detectable trace of oxygen in our Sn tower samples.

A small selection of AFM images taken *in situ* during the electrochemical reaction of Li with a patterned Sn electrode is given as Fig. 2. Positions of the displayed scans are indicated in the voltage profile at the bottom of Fig. 2. The AFM images show dark bands on both sides of the Sn tower. These dark bands (or shadows), that normally signify lower regions in the image, are artifacts from the AFM scanner.

The main component of an AFM scanner is a piezoelectric material used to position the cantilever on the sample. The tube-shaped piezoelectric material is fitted with five electrodes (one in the center and four on the outside). To move the cantilever over the sample, potentials are applied to the four electrodes. Unfortunately, the strain of the piezoelectric material is not directly proportional to the applied potential. Because of this, piezoelectric materials have an inherent hysteresis which causes “shadowing effects” to occur when the cantilever is raised over large surface features like the Sn towers.

The voltage curve at the bottom of Fig. 2 shows the evolution of the cell. As described in more detail elsewhere,<sup>13</sup> the cell was initially held at 0.8 V until the current reached 2 μA. Unfortunately, at this point, the cell was inadvertently shorted and was discharged to approximately 0.4 V after which the cell was cycled at a constant 2 μA between 0.0 and 1.3 V. During the last cycle the cell was charged to 2 V. The AFM images at the top of Fig. 2 show the evolution of the Sn tower as it reacts. As indicated by the vertical contrast scale in each image, inserting lithium into the electrode causes the tower to increase in height while removing lithium causes it to shrink. The images collected during this experiment were quantitatively analyzed using in-house image analysis software and the results are shown in Fig. 3.

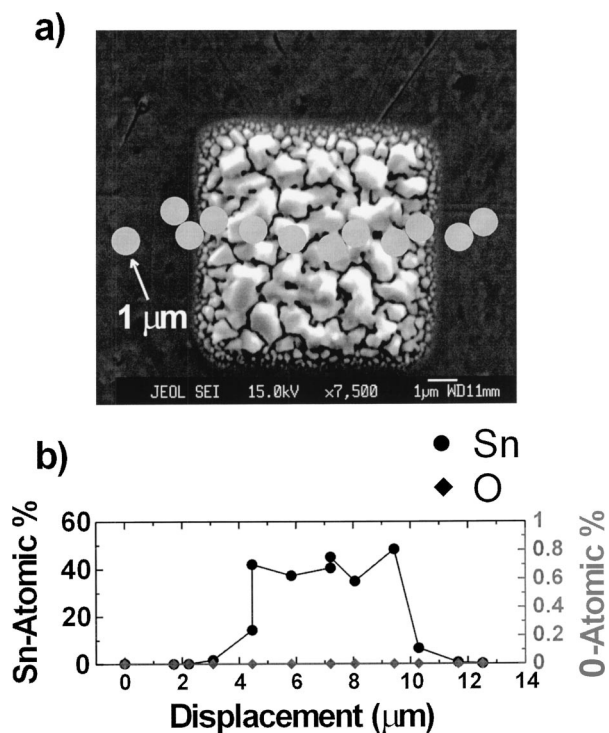


**Figure 1.** Electron probe analysis of a Sn tower. (a) Dots on the SEM micrograph show the approximate size and position of the electron-beam used to interrogate the sample. (b) Atomic percent of Sn and O in the Sn tower. The contributions of Fe and Cr are not shown.

Figure 3a shows the evolution of the width and length of the tower that is completely imaged in Fig. 2. Because the tower consists of a number of islands it was difficult to use our software to measure the length and width consistently. Despite this, it is still possible to see there is little change, if any, in the width and length of the tower correlated to the voltage curve. The change in average height and volume are shown in Fig. 3b and c, respectively. Both these parameters are directly related to the voltage curve shown in Fig. 3d. However, the electrode seems to be undergoing a continuous change in morphology during cycling. This can be understood because the electrode never returns to its initial condition. We speculate that this is caused by electrochemical pulverization of the tin particles. Large islands are broken into small, less-well packed ones, and hence the volume of the electrode steadily increases.

The constant change in the electrode surface can be observed from the AFM images collected at the top of charge (1.3 V). Figure 4 shows images 000 (a and b), 226 (c and d), and 449 (e and f) in two- and three-dimensional representations. Comparing these images shows that the islands making up the Sn tower become dilated in size as they press against each other. Similarly, the three-dimensional images (all shown with the same vertical scale and orientation), show how the height of the electrode is also increasing.

The experiment described by Fig. 2-4 shows that the morphology changes of patterned crystalline tin electrodes are not reversible.

*The reaction of Li with Al.*—Pure Al has also been investigated as a possible anode material for Li-ion batteries.<sup>15-17</sup> Al can react with Li to form LiAl, giving a specific capacity of 990 mAh/g. However, as for most pure crystalline elements, Al has very poor capacity retention.

The first *in situ* AFM study of the reaction of Li with Al was performed using a continuous thin Al film (0.5 μm thick) sputtered on the polished stainless steel substrates. Figure 5 shows the results of an *in situ* AFM experiment conducted on an Al electrode as it reacts with Li. Figure 5a shows a small selection of the AFM images collected during the experiment while Fig. 5b shows the voltage vs.

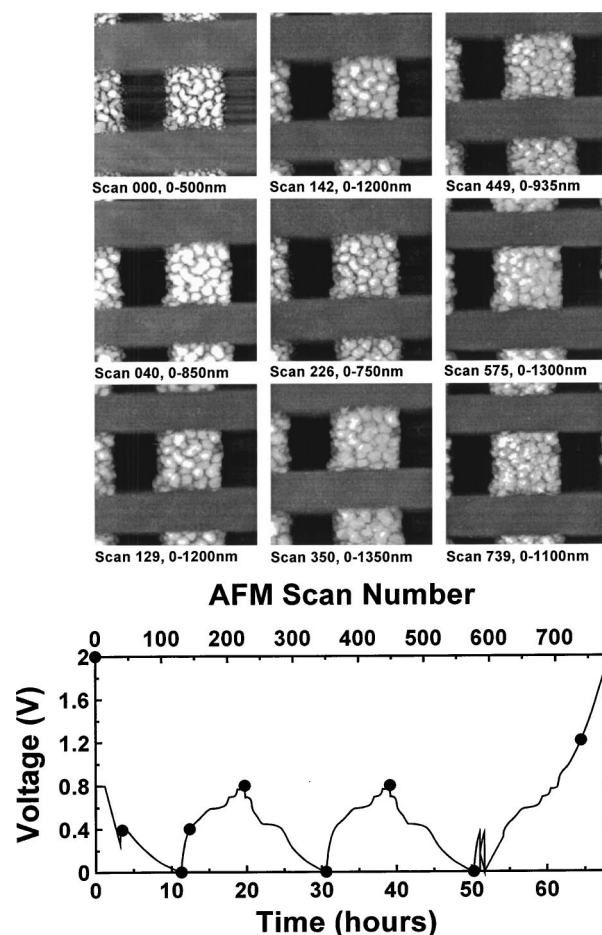


**Figure 2.** *In situ* AFM images taken during the electrochemical reaction of Li with patterned Sn. AFM images show the evolution of the Sn tower. (●) The point at which each AFM image was taken shown on the voltage vs. both time and AFM scan number.

time (bottom abscissa) and AFM scan number (top abscissa). The full reaction of Li with Al is available for viewing as a “time-lapsed movie” on the web site [www.physics.dal.ca/~dahn/ECS\\_Paper.html](http://www.physics.dal.ca/~dahn/ECS_Paper.html). Each AFM image is approximately  $24 \times 24 \mu\text{m}$  in size.

The electrode was initially discharged to 0.5 V for the first few cycles. We do not believe that a substantial amount of lithium reacts with the film during this portion of the experiment, given the known Li/Al voltage profile.<sup>15-17</sup> Images 000 and 117 show that the electrode surface is virtually unchanged during these cycles above 0.5 V. Then the electrode was allowed to discharge completely to 0 V. As shown by the vertical contrast scales of the images after number 117, allowing Li to react with the Al causes the film to expand vertically. Image 145 shows that the surface morphology of the electrode changes as more lithium is allowed to react with the Al film. This image shows, for the first time, the appearance of small “spikes” forming on the surface of the electrode. These spikes resemble triangles, which we believe are the image of the tip as it strikes sharp protrusions emanating from the electrode surface. As more Li is allowed to react with the film the number of spikes increases, as shown in image 161. Further reaction with Li causes the surface of the electrode to change as the spikes become larger. We believe that these spikes are caused by the nucleation of LiAl crystallites that are forced out of the surface of the film because they cannot fit within the film because of their larger size. The two-phase nature of the Al to LiAl reaction is responsible for this behavior.

Figure 6 shows cross sections of the surface of the Al film at scans 0, 161, and 222 during the discharge shown in Fig. 5. Dra-

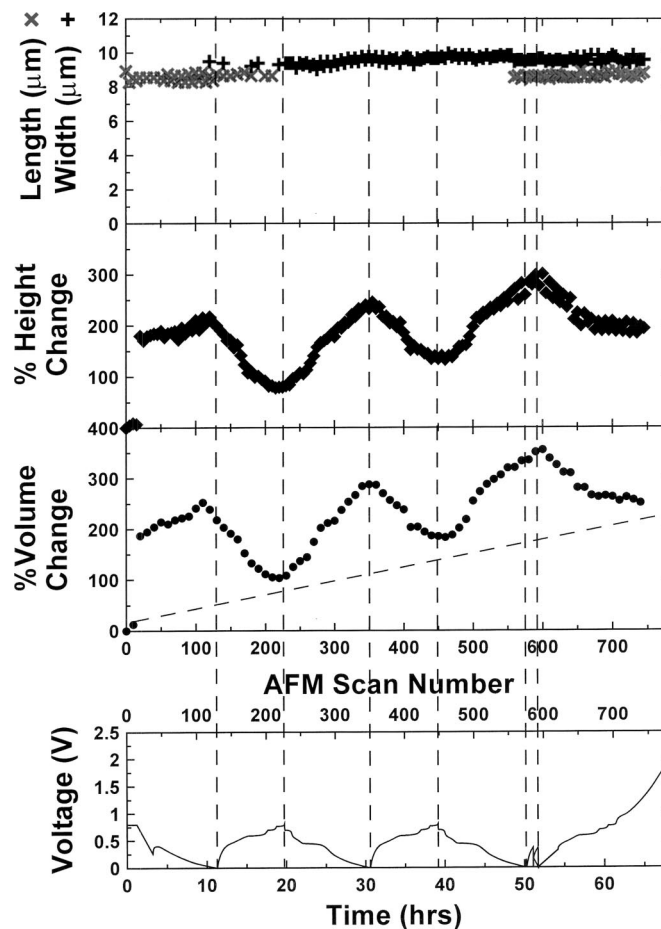


**Figure 3.** Analysis of the AFM images collected during the experiment shown in Fig. 2: (a) change in area, (b) percentage change in height, (c) percentage change in volume of the Sn tower, and (d) cell voltage vs. both time and AFM scan number.

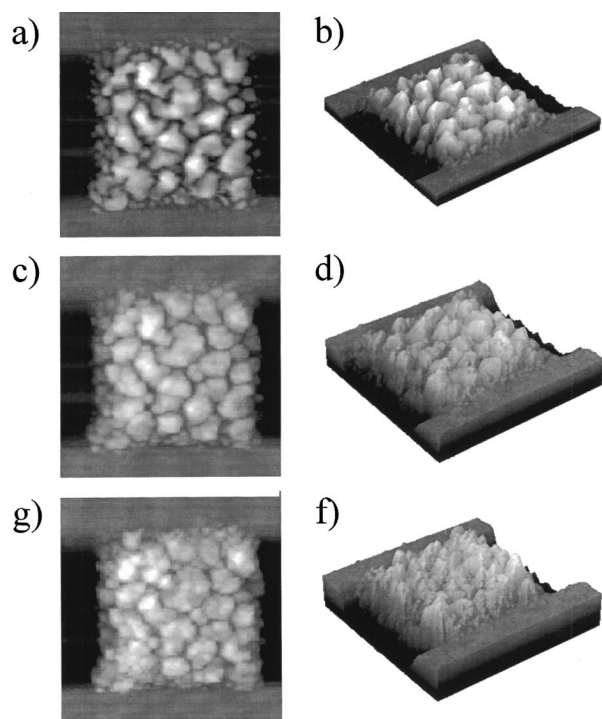
matic changes to the surface morphology and roughness of the film are evident as the Li-Al crystallites begin to form. Figure 7 shows a  $10 \times 10 \mu\text{m}$  portion of AFM images 000 and 161. As can be seen from images 7a and c, the density of spikes is much larger than is observable from the larger image. Images 7b and d show the three-dimensional representation of images 7a and c, respectively. The three-dimensional images show the changes to the electrode more clearly.

Other experiments performed on continuous Al films have shown similar results as observed here. Spikes on the surface of the Al electrode due to the nucleation of LiAl crystallites form when the voltage curve reaches the 0.2 V plateau.

*The reaction of Li with amorphous Si.*—Samples of patterned a-Si were sputtered on highly polished stainless steel substrates. Figure 8 shows the voltage vs. capacity for an a-Si electrode cycled vs. Li metal. The voltage curve of a-Si is very different than that of Al or Sn. The voltage profile of a-Si is smooth and continuous, indicating the absence of coexisting phase regions.

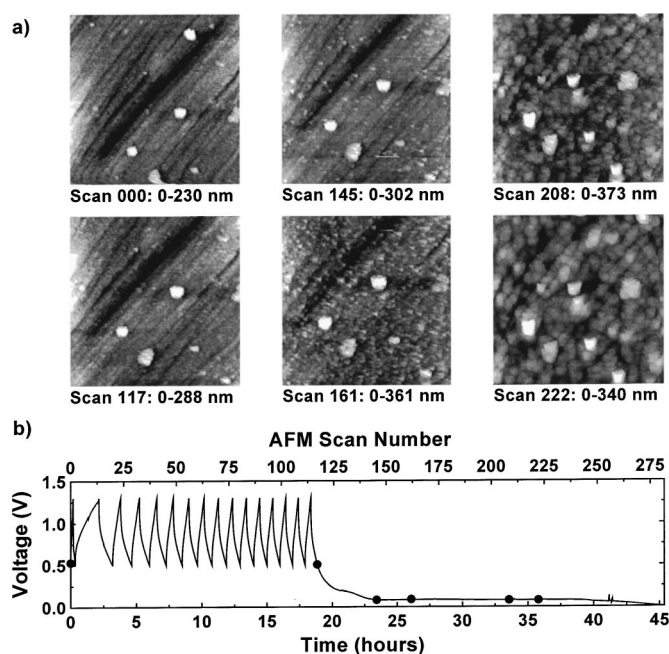
Because Si readily reacts with oxygen, WDS was used to search for oxygen in our a-Si samples. Similar to Sn, only a minute amount of oxygen (<1%) in the sample was detected.

Figure 9 shows topographic images taken during an *in situ* AFM experiment performed on a Li/a-Si cell. In order to view the towers more easily, the AFM topographs have only been tilted instead of flattened. The maximum value of the contrast scale as well as the approximate height of each tower is given in Table I. The a-Si towers appear to be smooth at all states of charge and show virtually no



**Figure 4.** Selected AFM images from Fig. 3 show the change in morphology of the Sn tower. Two- and three-dimensional images, respectively, of (a,b) scan 000, (c,d) scan 226, and (e,f) scan 449.

lateral changes caused by the reaction with Li. Because the vertical contrast scales of these AFM topographs are all from dark (minimum height) to light (maximum height), it is not possible to observe the change in height of the tower. This information can be obtained from a quantitative analysis of the AFM topographs.



**Figure 5.** Results of an *in situ* AFM experiment conducted on an Al film as it reacts with Li. (a) AFM topographs collected during the discharge. Each image is approximately  $24 \times 24 \mu\text{m}$  in size. The vertical contrast scale is indicated below each image. (b) Voltage vs. both time and AFM scan number collected during the experiment.

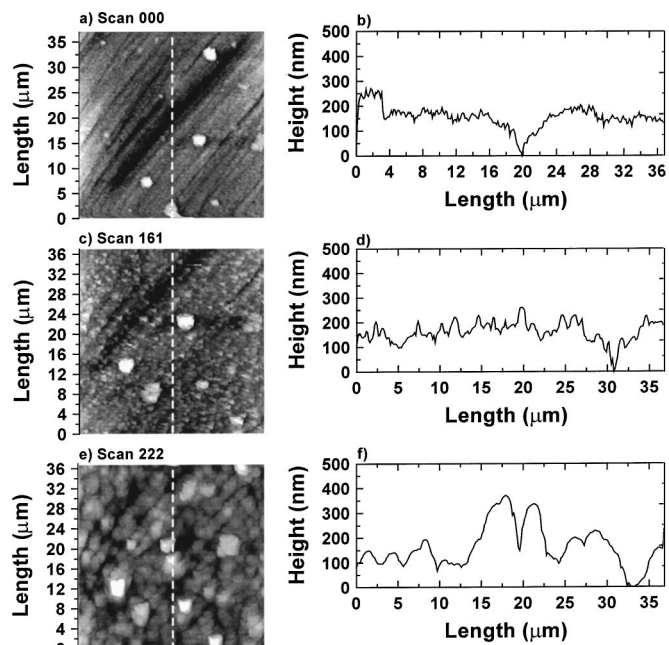


**Figure 6.** Cross sections of the AFM images 000, 161, and 222 collected during the discharge of the Li/Al cell described by Fig. 5.

Figure 10 shows the results from the analysis of the *in situ* AFM experiment shown in Fig. 9. Figure 10a-c shows the change in area, height, and volume, respectively, undergone by the tower during the reaction with lithium compared to the voltage profile shown in Fig. 10d. The first discharge (10d) shows a spurious capacity during which no change in height or volume is detected. As we discuss later, this irreversible capacity may be caused by various components of the wet-cell. The fact that there is no change in either height or volume during that time makes this argument probable. After the

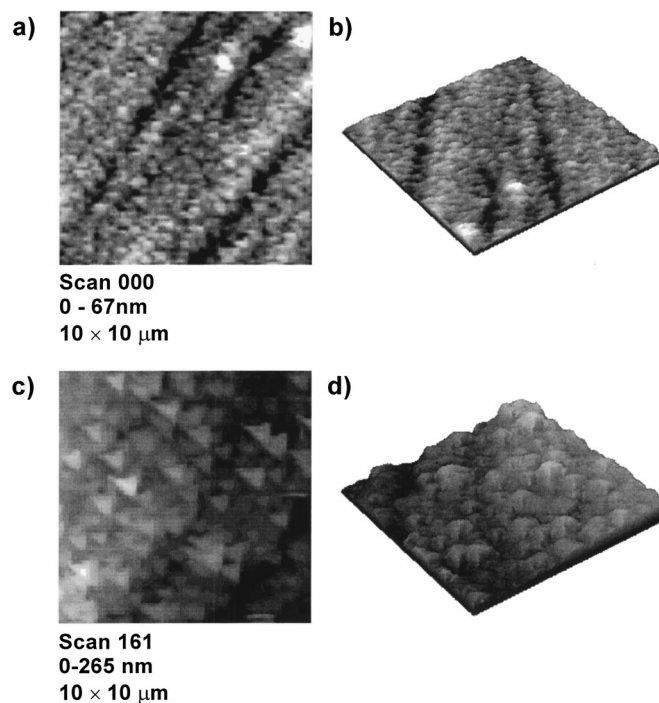


**Figure 7.** Two- and three-dimensional AFM images, respectively, of a  $10 \times 10 \mu\text{m}$  portion of the AFM images (a,b) 000 and (c,d) 161 from Fig. 5.

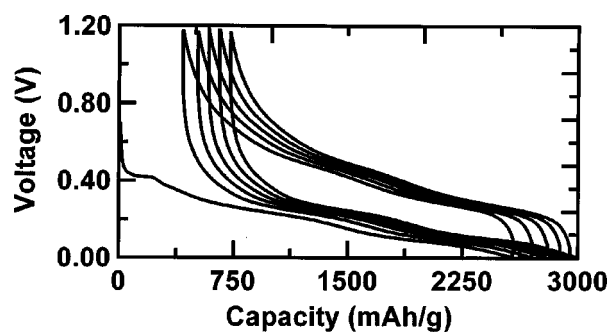


Figure 8. Voltage vs. capacity of a Li/a-Si cell.

first 50 AFM scans, the change in height and volume are direct functions of the lithium content in the electrode. Figure 10c also shows that the a-Si electrode almost returns to its initial volume after the first and second cycles. The change in volume of the electrode between 0.0 and 1.2 V is approximately 300%. In crystalline Si, each Si atom occupies a volume of  $20 \text{ \AA}^3$ . (Amorphous Si adopts a short-range diamond structure similar to crystalline Si. Therefore, assuming each Si atom occupies the same volume in a-Si as in crystalline Si is a fair approximation.) When crystalline Si reacts with Li to form  $\text{Li}_{4.4}\text{Si}$ , each Si atom occupies a volume of  $82 \text{ \AA}^3$ . This represents a 311% volume expansion. This value is consistent with that measured on a-Si in Fig. 10.

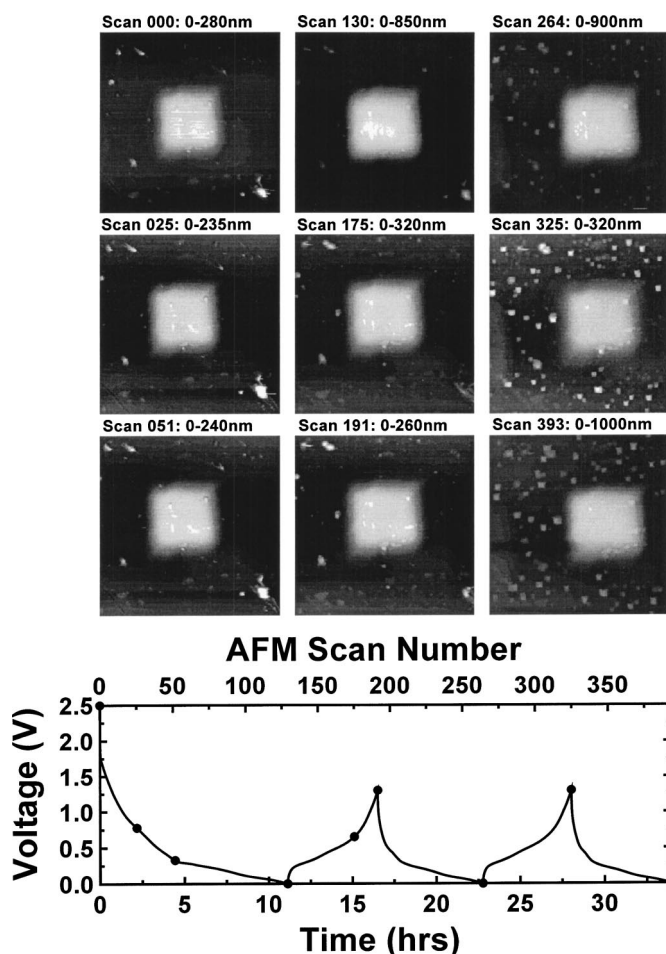


Figure 9. Topographic images obtained from an *in situ* AFM experiment on a patterned a-Si sample; (●) on the voltage vs. time and AFM scan number curve shows the state of charge where the AFM topographs were obtained.

Table I. Height changes of an a-Si tower as it reacts with Li as shown in Fig. 9.

AFM scan number	Maximum height of image (nm)	Approximate height of tower (nm)
000	280	210
025	235	215
051	240	221
130	850	757
175	320	303
191	260	249
264	900	742
325	320	254
393	1000	715

As mentioned previously, the first discharge of patterned a-Si cycled vs. Li is different from that of an a-Si film cycled vs. Li measured in a coin cell. As can be seen from Fig. 11, the voltage of the patterned electrode is much higher for the first half of the discharge. The discharge capacities in Fig. 11 have been normalized to 100% for both cells and the same scale factors have been applied to the charge curves. The charge of the electrode in the wet-cell is shorter than the discharge because of the high-voltage irreversible capacity. In a standard coin cell, approximately six drops of electrolyte are used, whereas in our wet-cell, approximately 1 mL of electrolyte (about 80 drops) is used. Furthermore, the patterned electrodes that we study have about 1/10 the electrode mass of a continuous film electrode used in a coin cell. Therefore, the effects of any electrolyte contaminant, like water, would be amplified at least 100-fold in our wet-cell. Thus, we believe the high voltage capacity during the first discharge in Fig. 9 and 11 is most likely caused by trace amounts of water in the electrolyte.

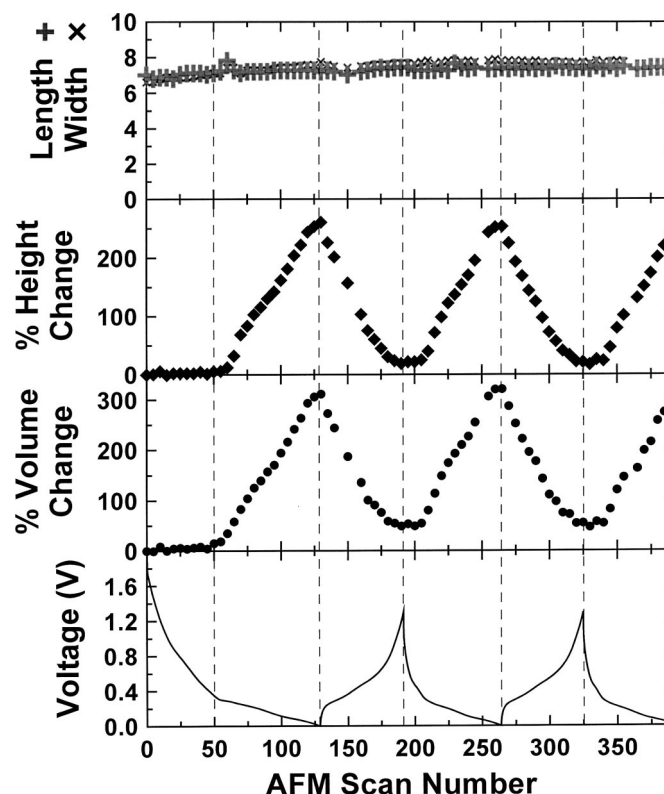
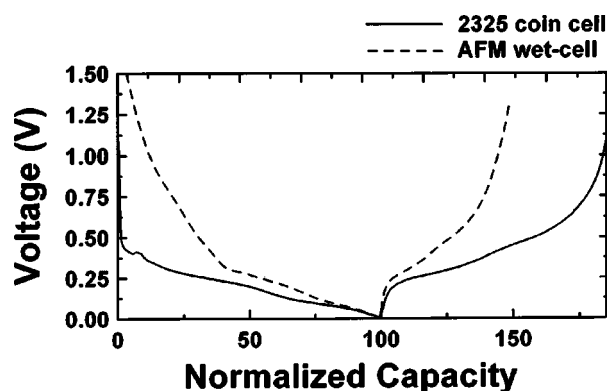


Figure 10. Change in (a) length + width, (b) height, and (c) volume of the a-Si tower shown in Fig. 6 compared to (d) voltage vs. AFM scan number.



**Figure 11.** Comparison between the voltage curve of a coin cell made from an a-Si film and an a-Si patterned electrode cycled in our AFM wet-cell.

Patterned a-Si electrodes that alloy with Li repeatedly have been shown to undergo reversible shape and morphology changes. These results differ markedly from the results reported above for crystalline Al and crystalline Sn. Reversible volume expansion on the order of 300% between a-Si and a-Li<sub>x</sub>Si at 0.0 V is observed.

*The reaction of Li with amorphous Si<sub>0.64</sub>Sn<sub>0.36</sub>.*—Patterned samples of a-Si<sub>0.64</sub>Sn<sub>0.36</sub> were prepared by sputter deposition as described previously. As discussed in greater detail in Ref. 7, sputtered samples of Si<sub>0.64</sub>Sn<sub>0.36</sub> are amorphous and adopted a short-range diamond structure similar to amorphous Si.

Figure 12 shows topographic images obtained from an *in situ* AFM experiment performed on a patterned a-Si<sub>0.64</sub>Sn<sub>0.36</sub> electrode cycled vs. Li metal. Each image is approximately 24 × 24 μm in size. The AFM image number and the vertical contrast scale is shown for each image. The voltage vs. time (bottom abscissa) and AFM scan number (top abscissa) is shown at the bottom of Fig. 12. The Li/Si<sub>0.64</sub>Sn<sub>0.36</sub> cell was initially discharged to 0.0 V and then held at 0.01 V for 1 h to ensure maximum capacity. The solid dots on the voltage curves indicate the positions where the AFM images were taken. As for the case with the Sn tower, the images show the effects of the piezo hysteresis discussed previously. Unlike Sn, the surface of the a-Si<sub>0.64</sub>Sn<sub>0.36</sub> tower is smooth and flat and shows no change in morphology due to the reaction with lithium. The only change shown by the a-Si<sub>0.64</sub>Sn<sub>0.36</sub> tower is in the direction perpendicular to the substrate. The reaction of Li with an a-Si<sub>0.64</sub>Sn<sub>0.36</sub> tower is available for viewing as a “time-lapsed movie” on the web site [www.physics.dal.ca/~dahn/ECS\\_Paper.html](http://www.physics.dal.ca/~dahn/ECS_Paper.html).

Figure 13 shows cross sections of some of the AFM images taken during the charge and discharge of the a-Si<sub>0.64</sub>Sn<sub>0.36</sub> electrode. Scans 000, 344, and 673 were all measured with the electrode either fresh or charged to 1.2 V. Scans 187 and 515 were measured in the fully discharged state. The height of the tower and its surface roughness does not change appreciably for the charged electrodes. In these cases the tower is about 220 nm high. By contrast, in the discharged state, the tower is about 600 nm high.

Figure 14 shows the quantitative analysis of the *in situ* experiment shown in Fig. 12. Figure 14a shows the change in area of the tower as a function of AFM scan number. Because of the surface features on the left side of the tower, it was not possible to obtain a reliable measure of the width of the tower. Therefore, the area shown in Fig. 14a is calculated from the measured height and volume. Little change is observed in the lateral dimensions of the tower. Figure 14b shows the change in height undergone by the tower during the electrochemical reaction with lithium. The change in height depends linearly on the lithium content in the electrode. Figure 14c shows the change in volume of the tower during the electrochemical reaction with lithium. The change in volume is also a linear function of the lithium content.

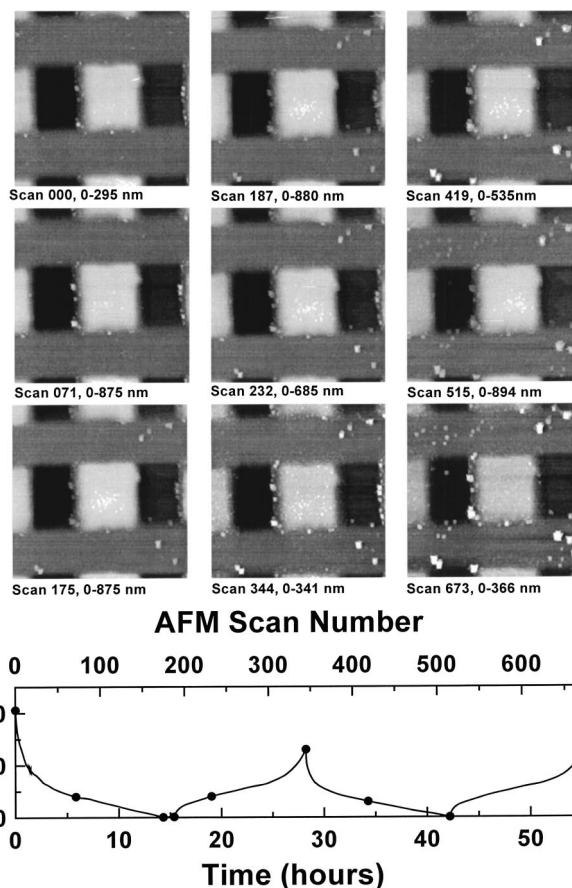


**Figure 12.** Topographic images obtained from an *in situ* AFM experiment on a patterned a-Si<sub>0.64</sub>Sn<sub>0.36</sub> sample; (●) on the voltage vs. time and AFM scan number curve shows the position where the AFM topographs were obtained.

Close inspection of Fig. 14 shows that the electrode's height and volume increases while the electrode is held fixed at 0.01 V. This suggests that the electrode does not initially reach its full capacity. In order to verify this, *in situ* AFM measurements were performed on another Li/Si<sub>0.64</sub>Sn<sub>0.36</sub> cell discharged to 0.0 V and held at 0.01 V for 8 h. In order to assess the ability of Li to diffuse into a-Si<sub>0.64</sub>Sn<sub>0.36</sub>, the cell was discharged at a relatively large current of 10 μA, which led to a 5 h discharge. Figure 15 shows the change in volume (15a) compared to the voltage curve (15b) both plotted vs. time (bottom abscissa) and AFM scan number (top abscissa). The electrode reaches a change in volume of approximately 250% after the initial constant current portion of the discharge. During the equilibration, the volume change of the a-Si<sub>0.64</sub>Sn<sub>0.36</sub> tower slowly increases to almost 300%. This shows that thin films of a-Si<sub>0.64</sub>Sn<sub>0.36</sub> reach most of their full capacity even when discharged at a C/5 rate. The volume expansion measured in this experiment agrees very well with that reported in Fig. 14.

Figure 14b and c shows that the change in height and volume of the tower does not go to zero once the lithium has been extracted from the electrode. However, the volume and morphology changes are very reversible in comparison to the changes observed for crystalline Al and Sn. This irreversible volume change may be due to some Li atoms which have remained trapped inside the a-Si<sub>0.64</sub>Sn<sub>0.36</sub> tower or the growth of a solid electrolyte interface (SEI) which is known to form on anode materials during cycling.

Close attention to Fig. 9 and 12 show that spikes form on the stainless steel substrate during the charge-discharge cycling. Moreover, the height and number of these spikes increase with increasing cycle number. An analysis was performed on the AFM images

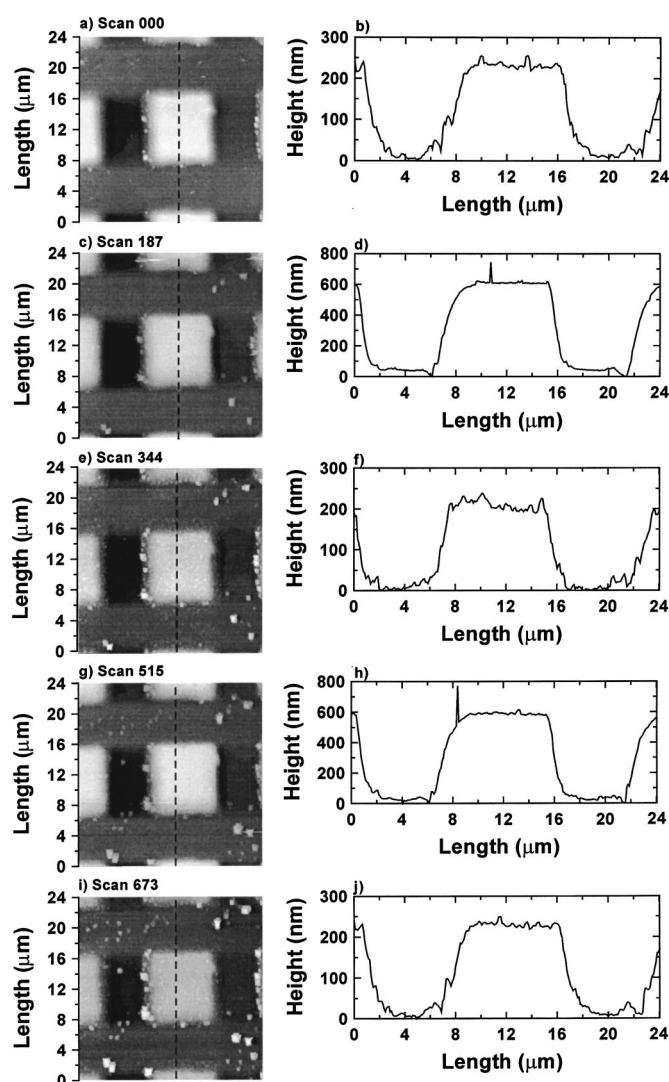


Figure 13. Cross sections of the AFM images 000, 187, 344, 515, and 673 collected during the discharge of the Li/a-Si<sub>0.64</sub>Sn<sub>0.36</sub> cell described by Fig. 12.

shown in Fig. 12. Figure 16a shows AFM image 673 from Fig. 12. The height and volume of the spikes indicated by arrows were measured as a function of state of charge, and the results are shown in Fig. 16b and c, respectively, compared to the voltage curve in Fig. 16d. Figure 16b and c show that the spikes only change during the initial stages of the discharge cycle. Furthermore, the spikes are found only to grow in size. These data imply that the spikes occur via an irreversible reaction similar to the formation of a SEI. We speculate that these spikes are the result of electrolyte decomposition at the surface of the substrate, perhaps on an imperfection in the oxide covering the stainless steel. We stress that these spikes are not of the same origin as the spikes that form due to the creation of LiAl on the Al towers in Fig. 5. In that case the spikes, caused by LiAl crystallites, form everywhere on the Al tower itself, while the spikes that form in Fig. 9 and 12 form away from the a-Si and a-Si<sub>0.64</sub>Sn<sub>0.36</sub> towers in random locations on the substrate, suggesting that they have nothing to do with the alloy reaction.

The AFM topographs in Fig. 12 show that the a-Si<sub>0.64</sub>Sn<sub>0.36</sub> tower does not undergo any cracking. These results, which are similar to those presented in Ref. 6 on the study of a-Si<sub>0.64</sub>Sn<sub>0.36</sub> thin films, show that particles of a-Si<sub>0.64</sub>Sn<sub>0.36</sub> can reversibly react with Li while undergoing volume changes on the order of 250%.

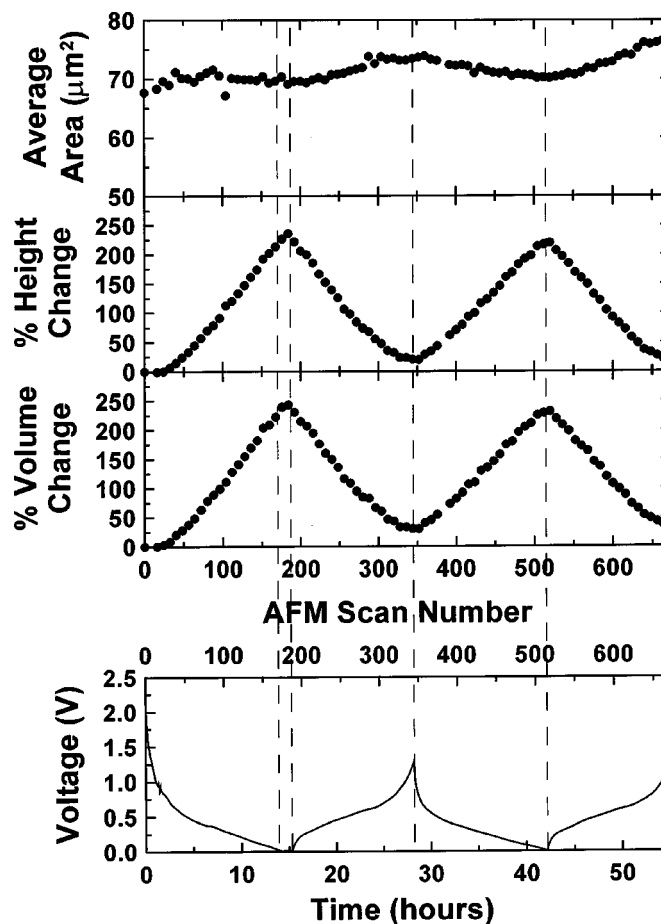


Figure 14. Analysis of an *in situ* AFM experiment on a patterned a-Si<sub>0.64</sub>Sn<sub>0.36</sub> electrode cycled vs. Li: (a) the change in area, (b) percent change in height, (c) percent change in volume, and (d) voltage vs. time and AFM scan number.

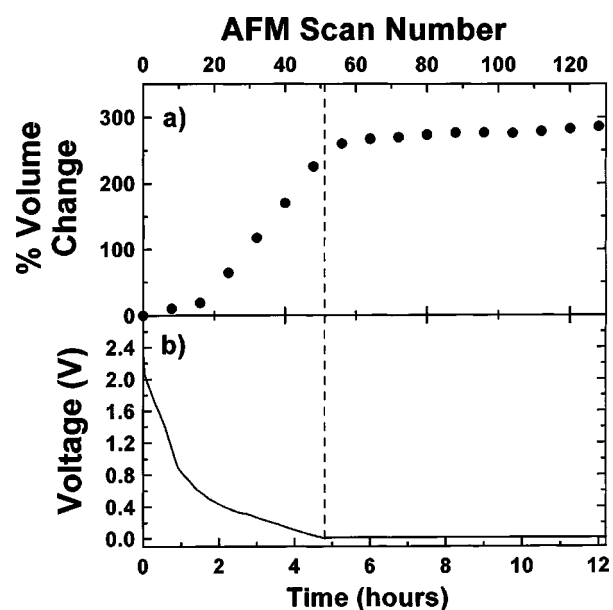
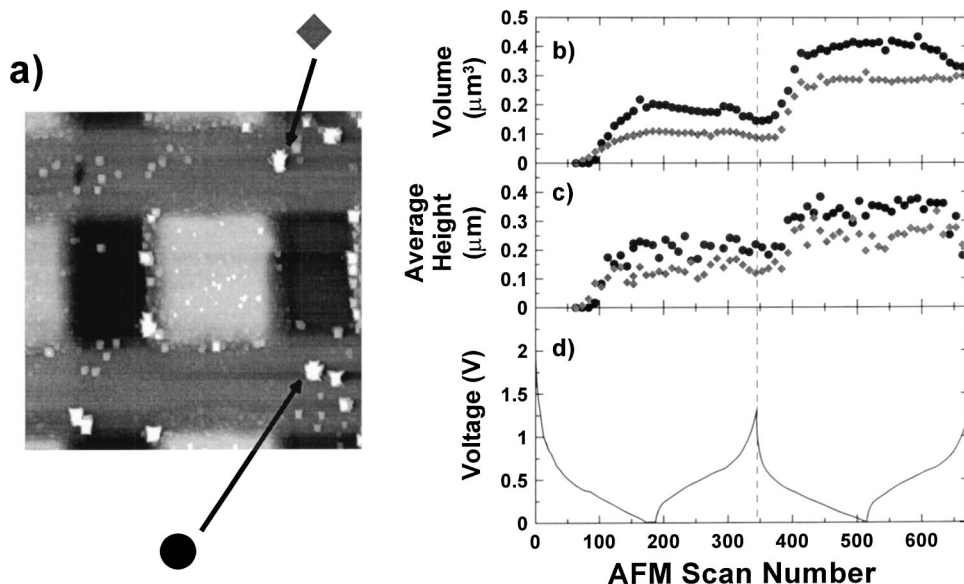


Figure 15. (a) Change in volume of a a-Si<sub>0.64</sub>Sn<sub>0.36</sub> tower and (b) voltage curve of a Li/a-Si<sub>0.64</sub>Sn<sub>0.36</sub> cell plotted vs. time and AFM scan number.



**Figure 16.** (a) AFM topograph number 673 from Fig. 12, (b) change in volume, (c) height of the two spikes shown in (a), and (d) voltage vs. AFM scan number for the Li/a-Si<sub>0.64</sub>Sn<sub>0.36</sub> cell.

### Conclusions

In this paper we have shown how the volume changes of patterned alloy electrodes as they react with lithium can be measured by AFM. It is surprising that brittle solids like a-Si and a-Si<sub>0.64</sub>Sn<sub>0.36</sub> can reversibly react with Li and undergo volume changes on the order of 250%. As mentioned in other work,<sup>6</sup> the expansions and contractions of these materials are completely analogous to the swelling of polymers by absorbed solvents. In both cases, additional atoms or molecules are incorporated homogeneously within the solid or polymer host, causing the expansion. In the case of patterned thin films of a-Si and a-Si<sub>0.64</sub>Sn<sub>0.36</sub>, the expansions are primarily in film thickness because of the good adhesion of the film to the rigid substrate. The same situation occurs in swelling polymers well bonded to rigid substrates.

One cannot overemphasize the contrasting behavior observed in the amorphous materials that show reversible morphology changes and the crystalline materials that do not. The crystalline materials Al and Sn show inhomogeneous volume expansion due to coexisting phase regions that lead to severe morphology changes and presumably is the cause of the poor capacity retention in Li/Al and Li/Sn cells.

The measurements on a-Si and a-Si<sub>0.64</sub>Sn<sub>0.36</sub> presented here along with those presented elsewhere<sup>6,9,13</sup> show that amorphous intermetallic materials can probably be optimized for use as anode materials in lithium-ion batteries. Based on the authors' private communications and many papers presented at lithium-ion battery conferences, some researchers in the lithium-ion battery community believe that there is no future for intermetallic electrodes. This opinion is based on the countless reports of crystalline intermetallic systems which, similar to Sn and Al electrodes, suffer from poor capacity retention due to self-pulverization. We believe the observations made in this work will put an end to the speculations that intermetallic materials are inherently unsuitable for application as anode materials for lithium-ion batteries. This, we hope, will spark a new wave of research on amorphous alloys in the same way that initial reports of tin-oxide materials<sup>18</sup> fueled the initial studies on tin-based and other alloy electrodes.

### Acknowledgments

The authors acknowledge support of this research by 3M Canada Company and the Natural Sciences and Engineering Research Coun-

cil (NSERC) of Canada. L.B., M.F., and T.H. acknowledge NSERC for scholarship support. L.B. also acknowledges 3M Canada for scholarship support. The authors also acknowledge numerous useful discussions with Larry Krause, Leif Christensen, Kevin Eberman, and Bob Turner.

*Dalhousie University assisted in meeting the publication costs of this article.*

### References

- C. J. Wen and R. A. Huggins, *J. Electrochem. Soc.*, **128**, 1181 (1981).
- J. Wang, I. D. Raistrick, and R. A. Huggins, *J. Electrochem. Soc.*, **133**, 457 (1986).
- J. Yang, M. Wachtler, M. Winter, and J. O. Besenhard, *Electrochim. Solid-State Lett.*, **2**, 161 (1999).
- I. A. Courtney, J. S. Tse, O. Mao, J. Hafner, and J. R. Dahn, *Phys. Rev. B*, **58**, 15583 (1998).
- For review see: M. Winter and J. O. Besenhard, *Electrochim. Acta*, **45**, 31 (1999); R. A. Huggins, in *Handbook of Battery Materials*, J. O. Besenhard, Editor, Part III, Chap. 5, Wiley-VCH, Weinheim (1999).
- L. Y. Beaulieu, K. W. Eberman, L. J. Krause, and J. R. Dahn, *Electrochim. Solid-State Lett.*, **4**, A137 (2001).
- L. Y. Beaulieu, K. C. Hewitt, R. L. Turner, A. Bonakdarpour, A. A. Abdo, K. W. Eberman, L. J. Krause, and J. R. Dahn, *J. Electrochem. Soc.*, *Accepted for publication*, (2002).
- L. Y. Beaulieu, T. D. Hatchard, and J. R. Dahn, Poster 251 presented at the 11th International Meeting on Lithium Batteries, Monterey, CA (2002).
- K. Sayama, H. Yagi, Y. Kato, S. Matsuta, H. Tarui, and S. Fujitani, Poster 52 presented at the 11th International Meeting on Lithium Batteries, Monterey, CA (2002).
- S. D. Beattie and J. R. Dahn, Abstract 275, The Electrochemical Society Meeting Abstracts, Vol. 2001-2, San Francisco, CA, Sept 2-7, 2001.
- S. D. Beattie and J. R. Dahn, *J. Electrochem. Soc.*, *Submitted*, (2002).
- N. Tamura, R. Ohshita, M. Fujimoto, S. Fujitani, M. Kamino, and I. Yonezu, *J. Power Sources*, **107**, 48 (2002).
- L. Y. Beaulieu, S. D. Beaulieu, T. D. Hatchard, and J. R. Dahn, *J. Electrochem. Soc.*, *Submitted*, (2002).
- L. Y. Beaulieu, V. K. Cumyn, K. W. Eberman, L. J. Krause, and J. R. Dahn, *Rev. Sci. Instrum.*, **72**, 3313 (2001).
- A. N. Dey, *J. Electrochem. Soc.*, **118**, 1547 (1971).
- J. O. Besenhard, *J. Electroanal. Chem. Interfacial Electrochem.*, **94**, 81 (1978).
- J. O. Besenhard, M. Hess, and P. Komenda, *Solid State Ionics*, **40**, 525 (1990).
- Y. Idota, T. Kubota, A. Matsufuji, A. Maekawa, and T. Miyasaki, *Science*, **276**, 1394 (1997).